

Group 4 Metallocene-Alumoxane Olefin Polymerization Catalysts. CPMAS-NMR Spectroscopic Observation of "Cation-like" Zirconocene Alkyls

Chand Sishta, Robin M. Hathorn, and Tobin J. Marks*

Department of Chemistry, Northwestern University
Evanston, Illinois 60208
Received August 16, 1991

The reaction products of group 4 metallocene dialkyls with oligomeric, partially hydrolyzed trimethylaluminum (methylalumoxane, MAO) constitute an extremely active and important, yet poorly understood class of homogeneous olefin polymerization catalysts.¹⁻³ Although XPS,⁴ surface chemical,⁵ model synthetic,⁶⁻¹⁰ and theoretical studies¹¹ suggest indirectly that the primary role of the Lewis acidic^{1f,3} alumoxane may be alkide abstraction to afford unsaturated "cation-like" catalytic centers (e.g., **A** in eq 1, Cp = $\eta^5\text{-C}_5\text{H}_5$),⁴⁻¹⁰ alternative proposals have been made,^{1a,f,g,2} and more direct structure/reactivity information would

$$\text{Cp}_2\text{Zr}(\text{CH}_3)_2 + [\text{Al}(\text{CH}_3)_n\text{O}]_m \rightleftharpoons \text{Cp}_2\text{ZrCH}_3^+\{\text{CH}_3[\text{Al}(\text{CH}_3)_n\text{O}]_m\}^- \quad (1)$$

A

be highly desirable. Efforts to apply solution NMR spectroscopy to this problem are complicated by a complex variety of (temperature-dependent) equilibrium, chemical exchange,^{9b} and quadrupole relaxation processes^{1a,f,12} as well as, for in situ catalytic studies, the extremely high polymerization activity. We report here the application of solid-state CPMAS-NMR techniques to

(1) (a) Resconi, L.; Bossi, S.; Abis, L. *Macromolecules* **1990**, *23*, 4489-4491, and references therein. (b) Piccolrovazzi, N.; Pino, P.; Consiglio, G.; Sironi, A.; Moret, M. *Organometallics* **1990**, *9*, 3098-3105, and references therein. (c) Waymouth, R.; Pino, P. *J. Am. Chem. Soc.* **1990**, *112*, 4911-4914, and references therein. (d) Ewen, J. A.; Jones, R. L.; Razavi, A.; Ferrara, J. D. *J. Am. Chem. Soc.* **1988**, *110*, 6255-6256, and references therein. (e) Kaminsky, W.; Kulper, K.; Brintzinger, H. H.; Wild, F. R. W. *Angew. Chem., Int. Ed. Engl.* **1985**, *24*, 507-508, and references therein. (f) Giannetti, E.; Nicoletti, G. M.; Mazzocchi, R. *J. Polym. Sci., Polym. Chem. Ed.* **1985**, *23*, 2117-2133, and references therein. (g) Kaminsky, W.; Miri, M.; Sinn, H.; Woldt, R. *Makromol. Chem. Rapid Commun.* **1983**, *4*, 417-421. (h) Sinn, H.; Kaminsky, W.; Vollmer, H.-J.; Woldt, R. *Angew. Chem., Int. Ed. Engl.* **1980**, *19*, 390-392.

(2) Sinn, H.; Kaminsky, W. *Adv. Organomet. Chem.* **1980**, *18*, 99-149.

(3) For information on the structures of methylalumoxane and related compounds, see refs 1a,f and the following: (a) Bott, S. G.; Coleman, A. W.; Atwood, J. L. *J. Am. Chem. Soc.* **1986**, *108*, 1709-1710. (b) Atwood, J. L.; Hrnrcid, D. C.; Priester, R. D.; Rogers, R. D. *Organometallics* **1983**, *2*, 985-989. (c) Lasserre, S.; Derouault, J. *Nouv. J. Chim.* **1983**, *7*, 659-665. (d) Boleslawski, M.; Serwatowski, J. *J. Organomet. Chem.* **1983**, *254*, 159-166. (e) Pastnkiewicz, S. *Polyhedron* **1990**, *9*, 429-453. (f) Aoyagi, T.; Araki, T.; Oguni, N.; Mikumo, M.; Tani, H. *Inorg. Chem.* **1973**, *12*, 2702-2707.

(4) Gassman, P. G.; Callstrom, M. R. *J. Am. Chem. Soc.* **1987**, *109*, 7875-7876.

(5) Dahmen, K. H.; Hedden, D.; Burwell, R. L., Jr.; Marks, T. J. *Langmuir* **1988**, *4*, 1212-1214.

(6) (a) Jordan, R. F.; Taylor, D. F.; Baenziger, N. C. *Organometallics* **1990**, *9*, 1546-1557. (b) Jordan, R. F.; LaPointe, R. E.; Bradley, P. K.; Baenziger, N. *Organometallics* **1989**, *8*, 2892-2903. (c) Jordan, R. F.; Echols, S. F. *Inorg. Chem.* **1987**, *26*, 383-386. (d) Jordan, R. F.; LaPointe, R. E.; Bajgur, C. S.; Echols, S. F.; Willett, R. J. *J. Am. Chem. Soc.* **1987**, *109*, 4111-4113. (e) Jordan, R. F.; Bajgur, C. S.; Dasher, W. E.; Rheingold, A. L. *Organometallics* **1987**, *6*, 1041-1051. (f) Jordan, R. F.; Bajgur, C. S.; Willett, R.; Scott, B. J. *J. Am. Chem. Soc.* **1986**, *108*, 7410-7411. (g) Jordan, R. F.; Dasher, W. E.; Echols, S. F. *J. Am. Chem. Soc.* **1986**, *108*, 1718-1719.

(7) (a) Bochmann, M.; Jagger, A. J.; Nicholls, J. C. *Angew. Chem., Int. Ed. Engl.* **1990**, *29*, 780-782, and references therein. (b) Bochmann, M.; Jagger, A. J.; Wilson, L. M.; Hursthouse, M. B.; Motevalli, M. *Polyhedron* **1989**, *8*, 1838-1843.

(8) (a) Hlatky, G. G.; Turner, H. W.; Eckman, R. R. *J. Am. Chem. Soc.* **1989**, *111*, 2728-2729. (b) Taube, R.; Krukowka, L. *J. Organomet. Chem.* **1988**, *347*, C9-C11. (c) Eisch, J. J.; Piotrowski, A. M.; Brownstein, S. K.; Gabe, E. J.; Lee, F. L. *J. Am. Chem. Soc.* **1985**, *107*, 7219-7220.

(9) (a) Siedle, A. R.; Newmark, R. A.; Schroepfer, J. N.; Lyon, P. A. *Organometallics* **1991**, *10*, 400-404. (b) Siedle, A. R.; Newmark, R. A.; Lamanna, W. M.; Schroepfer, J. N. *Polyhedron* **1990**, *9*, 301-308.

(10) Yang, X.; Stern, C. L.; Marks, T. J., *J. Am. Chem. Soc.* **1991**, *113*, 3623-3625.

(11) (a) Jolly, C. A.; Marynick, D. S. *J. Am. Chem. Soc.* **1989**, *111*, 7968-7974. (b) Lauher, J. W.; Hoffmann, R. *J. Am. Chem. Soc.* **1976**, *98*, 1729-1742.

(12) Sishta, C.; Marks, T. J., unpublished results.

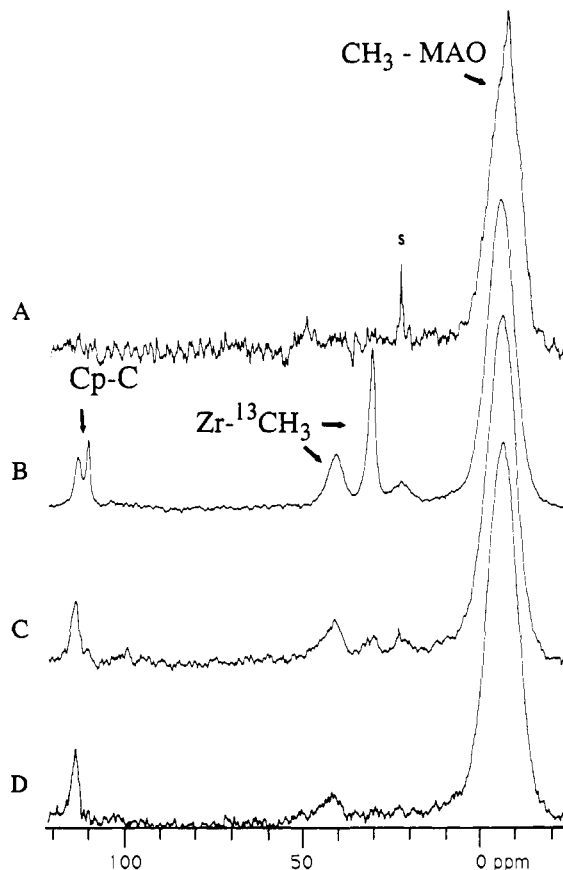


Figure 1. ^{13}C CPMAS-NMR spectra of (A) neat methylalumoxane (1024 scans), (B) the reaction product of methylalumoxane + $\text{Cp}_2\text{Zr}(\text{CH}_3)_2$ (Al:Zr = 5:1; 1024 scans), (C), as in Figure 1B with Al:Zr = 10:1 (1024 scans), (D) as in Figure 1B,C with Al:Zr = 20:1 (1024 scans). S = solvent.

the solid (immobilized) catalytic species and the direct observation, for the first time, of the formation and olefinic insertion reactivity of an MAO-stabilized "cation-like" zirconocene alkyl.

Using rigorously anhydrous and anaerobic glovebox/high vacuum line methodology,^{5,13} toluene solutions of MAO (Schering) were evaporated, and the resulting colorless powder was dried 12 h (25 °C) under high vacuum (to remove excess trimethylaluminum^{1a}). Various Al:Zr ratios of MAO: $\text{Cp}_2\text{Zr}(\text{CH}_3)_2$ (**1**, 99% ^{13}C)⁵ were weighed into a fritted reaction vessel, dissolved in toluene, stirred for 1 h,^{14a} and filtered; the filtrate was then evaporated, and the red-orange residue was dried under high vacuum for 12 h (25 °C). ^{13}C CPMAS-NMR spectroscopy of the resulting solids was carried out using methodology described elsewhere.^{13,14b} Control experiments including deliberate air exposure indicated negligible sample decomposition over the course of spectroscopic experiments.¹⁵

Figure 1A shows the ^{13}C CPMAS spectrum of MAO, which exhibits a single, broadened (at least partially quadrupolar in origin^{16,17}) $^{13}\text{CH}_3$ ^{27}Al signal¹⁶ at δ -6.5. Several features are evident in the spectrum of a $\text{Cp}_2\text{Zr}(\text{CH}_3)_2$ + MAO sample prepared with Al:Zr = 5:1 (Figure 1B). In addition to resonances characteristic of MAO (δ CH_3 unchanged from neat MAO) and

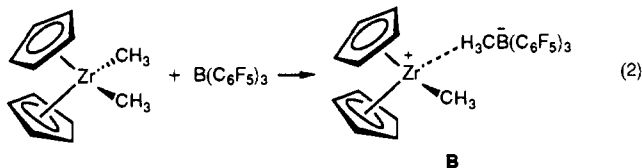
(13) (a) Finch, W. C.; Gillespie, R. D.; Hedden, D.; Marks, T. J. *J. Am. Chem. Soc.* **1990**, *112*, 6221-6232. (b) Hedden, D.; Marks, T. J. *J. Am. Chem. Soc.* **1988**, *110*, 1647-1649.

(14) (a) Solution NMR experiments¹² indicate that reaction is complete within ~5 min at -78 °C. (b) Varian VXR300 (75.45 MHz) with Doty high speed CPMAS probe; sapphire rotors with Kel-F endcaps, and boil-off nitrogen spinning gas. Typical optimized spectral parameters: repetition time, 4 s; CP time, 2.5 ms; spinning speed, 8 kHz. Chemical shifts were externally referenced to hexamethylbenzene (δ (^{13}C methyl) = 17.30 vs TMS).

(15) Air exposure immediately bleaches the catalyst color and an OCH_3 resonance¹¹ appears at δ 55.

(16) Toscano, P. J.; Marks, T. J. *J. Am. Chem. Soc.* **1985**, *107*, 653-659.

$\text{Cp}_2\text{Zr}(\text{}^{13}\text{CH}_3)_2$ (δ 31.7 (Zr-CH₃), 111.5 (Zr-Cp)),⁵ new downfield-shifted Zr-CH₃ and Zr-Cp signals are observed at δ 41.3 and 114.4, respectively. The Zr-CH₃ assignment of the former is confirmed by dipolar dephasing¹⁸ and parallel experiments with natural abundance **1** + MAO, which reveal identical spectral features but methyl signals which are appropriately diminished in intensity. The downfield Zr-CH₃ and Zr-Cp displacements are typical of "cation-like" $\text{Cp}_2\text{ZrR}^+/\text{Cp}_2\text{Zr(L)R}^+$ complexes,^{5,6,10,19,20} with the most revealing model being $\text{Cp}_2\text{ZrCH}_3^+ \text{CH}_3\text{B}(\text{C}_6\text{F}_5)_3^-$ (δ Zr-CH₃ = 40.9, δ Zr-Cp = 114.0 in C_6D_6 , 39.8 and 115.3 in the neat solid), prepared by stoichiometric methide abstraction using the organo-Lewis acid $\text{B}(\text{C}_6\text{F}_5)_3$ ¹⁰ (**B**, eq 2). **B** approaches $\text{Cp}_2\text{Zr}(\text{CH}_3)_2$ + MAO catalysts in polymerization activity.¹⁰ As the Al:Zr ratio in the $\text{Cp}_2\text{Zr}(\text{}^{13}\text{CH}_3)_2$ + MAO



solution phase reactions is increased, the CPMAS-NMR after solvent evaporation shows the "cation-like" $\text{Cp}_2\text{Zr}^{13}\text{CH}_3^+$ (**2**) features to increase at the expense of those due to **1** (Figure 1C,D). By Al:Zr \approx 12:1 signals due to complex **1** are no longer visible. Close comparison of the Zr-CH₃:Al-CH₃ intensities²¹ in Figure 1B-D versus those in neat $\text{Cp}_2\text{Zr}(\text{}^{13}\text{CH}_3)_2$ (with constant CP and other instrumental parameters) indicates that the ¹³CH₃ label has been scrambled completely among the MAO, $\text{Cp}_2\text{Zr}^{13}\text{CH}_3^+$, and $\text{Cp}_2\text{Zr}(\text{}^{13}\text{CH}_3)_2$ sites. Moreover, redissolution in toluene of a solid $\text{Cp}_2\text{Zr}(\text{}^{13}\text{CH}_3)_2$ + MAO sample (Al:Zr = 10:1), addition to this solution of 5 equiv of $\text{Cp}_2\text{Zr}(\text{CH}_3)_2$, evaporation, and CPMAS spectroscopy yields a cation/neutral intensity pattern compatible only with complete Zr-¹³CH₃/Zr-CH₃ scrambling. Clearly eq 1 is rapid in solution under the present experimental conditions.

To probe the polymerization activity of the proposed zirconocene cation, solid $\text{Cp}_2\text{Zr}(\text{}^{13}\text{CH}_3)_2$ + MAO product samples were dosed on a high vacuum line with measured quantities of rigorously purified¹³ ethylene at 77 K (30 min; to moderate activity and allow ethylene diffusion into the solid). The samples were then warmed to room temperature over a period of 1–2 h, and CPMAS spectra were recorded. For the Al:Zr = 5:1 sample, the result of incremental ethylene dosing (Figure 2) is diminution and ultimate disappearance (reaction) of the Zr-¹³CH₃⁺ feature relative to the Cp and MAO resonances. In addition, a feature grows in at δ 14.5 which can be assigned to the ¹³CH₃ terminus of an oligo-ethylene chain²² (possibly diminished in intensity due to mobility-related inefficiency of the CP process). An increase in the relative intensity in the Zr-¹³CH₃ region of **1**/MAO can be associated with the appearance of the magnetically coincident $(\text{CH}_2\text{CH}_2)_n$ resonances, expected at \sim δ 32.²² Confirmatory experiments using isotopically depleted (0.04% ¹³C) ethylene-¹²C₂ (Figure 2E,F) reveal complete diminution of the Zr-¹³CH₃⁺ signal upon ethylene dosing but insignificant (\pm 15%) decline in that of Zr-¹³CH₃ (**1**/MAO). We interpret these observations in terms

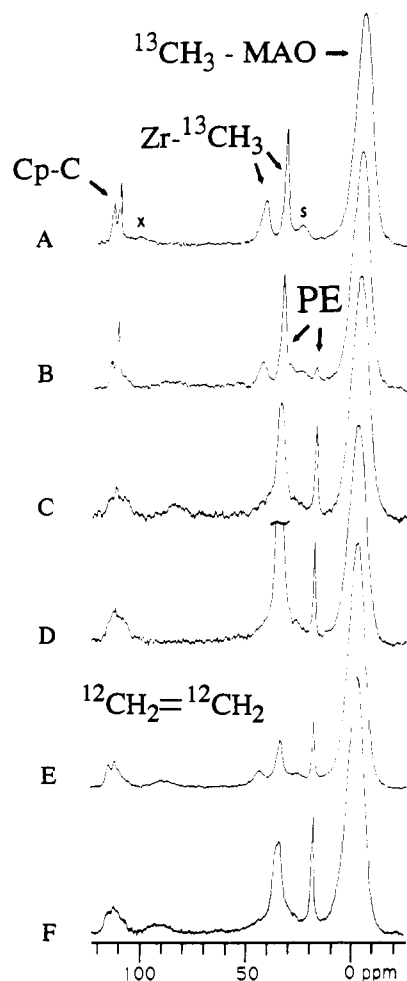
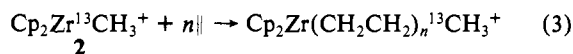


Figure 2. ¹³C CPMAS-NMR spectra of (A) reaction product of methylalumoxane + $\text{Cp}_2\text{Zr}(\text{}^{13}\text{CH}_3)_2$ (Al:Zr = 5:1; 1024 scans) dosed with 0.0 equiv (per Zr) of ethylene, (B) sample of Figure 2A dosed with 6.0 equiv (per Zr) of ethylene (1024 scans), (C) sample of Figure 2A dosed with 12.0 equiv (per Zr) of ethylene (2022 scans), (D) sample of Figure 2A dosed with 48.0 equiv (per Zr) of ethylene (1024 scans), (E) reaction product of methylalumoxane + $\text{Cp}_2\text{Zr}(\text{}^{13}\text{CH}_3)_2$ (Al:Zr = 6:1) dosed with 12.0 equiv (per Zr) of ethylene-¹²C₂ (99.96% ¹²C; 5120 scans), and (F) sample of Figure 2E dosed with 48.0 equiv (per Zr) of ethylene-¹²C₂ (99.96% ¹²C; 6223 scans). S = solvent; X = spinning sideband.

of sequential olefin insertion^{13,23,24} exclusively into the Zr-¹³CH₃ bond of the cation (eq 3). Consistent with this picture, the



chemical shift pattern in the 1/2 Cp region is largely unchanged (excepting some increase in line width), further confirming that **1**/MAO is unreactive toward, and not converted into, a cation by ethylene, while **2** evolves into a second cation (eq 3). Identical behavior is observed at higher Al:Zr ratios, except that the spectral features of **1** are of course absent. In regard to the rate of possible Zr-alkyl/Al-^{12,13}CH₃ exchange processes in the solid state, negligible changes in relative Zr-¹³CH₃ spectral intensities are observed over the course of 5 days (25 °C).²⁵

(17) (a) Harris, R. K.; Nesbitt, G. J. *J. Magn. Reson.* **1988**, *78*, 245–256. (b) Jonsen, P. *J. Magn. Reson.* **1988**, *77*, 348–355. (c) Olivieri, A. C.; Frydman, L.; Grasselli, M.; Diaz, L. E. *J. Magn. Reson.* **1988**, *76*, 281–289. (d) Naito, A.; Ganapathy, S.; McDowell, C. A. *J. Magn. Reson.* **1982**, *48*, 367–381.

(18) (a) Alemany, L. B.; Grant, D. M.; Alger, T. D.; Pugmire, R. J. *J. Am. Chem. Soc.* **1983**, *105*, 6697–6704. (b) Opella, S. J.; Frey, M. H. *J. Am. Chem. Soc.* **1979**, *101*, 5854–5856.

(19) (a) Other Zr¹³CH₃ data: $\text{Cp}_2\text{Zr}(\text{CH}_3)(\text{picoline})^+\text{BPh}_4^-$, δ 44.2 (Zr-Cp = 114.1);^{5a} $\text{Cp}_2\text{Zr}(\text{CH}_3)(\text{THF})^+\text{BPh}_4^-$, δ 38.9;⁵ $\text{Cp}_2\text{Zr}(\text{CH}_3)_2$ /dehydroxylated alumina, δ 35.9 (Zr-Cp = 112).⁵ In contrast, for $\text{Cp}_2\text{Zr}(\text{CH}_3)[\text{OCH}(\text{CH}_3)_2]$, δ 30.8.^{6c} (b) $\text{Cp}_2\text{Zr}(\text{CH}_3)(\text{NCCH}_3)^+$ complexes appear to be an exception (δ Zr-CH₃ \approx 31).^{5b}

(20) (a) δ Zr¹³CH₃ is usually in the δ 36–44-ppm region. (b) Zr(μ -¹³CH₃)Al resonances are expected at \sim δ -21.^{9a}

(21) Observed Cp: Σ CH₃ intensity ratios agree with theoretical to within \pm 20%, which is realistic assuming that CP efficiencies may vary somewhat with ¹³C nuclear environment.¹³

(22) Vander Hart, D. L.; Pérez, E. *Macromolecules* **1986**, *19*, 1902–1909.

(23) (a) Burger, B. J.; Thompson, M. E.; Cotter, W. D.; Bercaw, J. E. *J. Am. Chem. Soc.* **1990**, *112*, 1566–1577. (b) Brookhart, M.; Lincoln, D. M. *J. Am. Chem. Soc.* **1988**, *110*, 8719–8720. (c) Clawson, L.; Soto, J.; Buchwald, S. L.; Steigerwald, M. L.; Grubbs, R. H. *J. Am. Chem. Soc.* **1985**, *107*, 3377–3378.

(24) In principle, Zr-CH₂- resonances should be visible at δ 60–70,^{6b} however, lack of ¹³C enrichment (intensity should be \sim 10% of the 2-Cp signal) and the expected chemical shift dispersion^{6b} likely obscure these features.

(25) Similar observations are made if the sample in Figure 2D is dissolved in toluene and stirred for 6 h, the solvent is evaporated, and a CPMAS spectrum is recorded.

In summary, these results provide the first direct observation in the reaction between a metallocene dialkyl and methylaluminumoxane of a "cation-like" $\text{Cp}_2\text{ZrCH}_3^+$ species, the entirety of which undergoes facile ethylene insertion. These results also argue that the Al:Zr stoichiometry required for complete $1 \rightarrow 2$ conversion is considerably lower than employed in typical catalytic reactions.¹⁻³

Acknowledgment. We are grateful to the Division of Chemical Sciences, Office of Basic Energy Sciences, Office of Energy Research, U.S. Department of Energy, for support of this research under Grant DE-FG02-86ER13511. C.S. acknowledges the Dow Chemical Co. for a postdoctoral fellowship. We thank Dr. X. Yang for helpful discussions and Dr. J. C. Stevens of Dow Chemical for methylalumoxane samples.

Registry No. 1, 115942-68-2; ethylene, 74-85-1.

The Electron Momentum Density in the Highest Energy Occupied Molecular Orbital of Borazine, $\text{B}_3\text{N}_3\text{H}_6$: Evidence for Localization

J. A. Tossell* and J. H. Moore

Department of Chemistry and Biochemistry
University of Maryland
College Park, Maryland 20742

K. McMillan, C. K. Subramaniam, and M. A. Coplan

Institute for Physical Science and Technology
University of Maryland
College Park, Maryland 20742

Received June 19, 1991

Borazine, $\text{B}_3\text{N}_3\text{H}_6$, is often called an "inorganic benzene" implying it to be a highly conjugated molecule; however, the actual extent of borazine aromaticity remains an open issue.¹⁻⁴ Two of the outer occupied orbitals of borazine, $1a_2''$ and $1e''$, correlate with the two occupied π orbitals of benzene. Molecular orbital calculations indicate that the electron density associated with these orbitals is delocalized over the nitrogen and, to a lesser extent, the boron atoms.³ On the other hand, calculations using spin-coupled valence bond theory to introduce electron correlation have indicated that correlated π -electrons are better described in terms of semilocalized orbitals. An experimental test to discriminate between the delocalized Hartree-Fock and a more localized correlated description would be desirable.

To analyze the $1e''$ HOMO of borazine we have used (e,2e) spectroscopy.⁵⁻⁷ This technique involves the impulsive ejection of an electron from a molecule by electron impact with simultaneous determination of the energies and momenta of the ejected and scattered electrons. Energy and momentum conservation give the binding energy and momentum of the ejected electron at the instant of impact. When a sufficient number of (e,2e) events have been accumulated, the cross section for the ionization process as a function of the momentum of the ejected electron can be determined. Within the plane-wave impulse approximation, this cross section is proportional to the spherically averaged orbital electron momentum overlap density (OVD) between the neutral target and the residual cation. The OVD is in turn similar to, but not

Table I. Vertical Binding Energies (eV) of the Three Highest Valence MOs of Borazine

orbital	exptl BE, ^a eV	previous work ^b		present work	
		$-\epsilon_i$	ΔE_{UHF}^c	$-\epsilon_i$	$\Delta E_{\text{HF-CI}}^d$
$1e''(\pi)$	10.1	11.3	9.4	11.3	10.4
$6e'(\sigma)$	11.4	12.4	11.4	12.8	11.9
$1a_2''(\pi)$	12.8	14.1	13.0	14.2	13.2

^aReference 8. ^bReference 9. ^c ΔE_{UHF} is the difference in total energy at the UHF level between neutral molecule and cation. ^d $\Delta E_{\text{HF-CI}}$ is the difference in total energy at the HF-CI level between neutral molecule and cation.

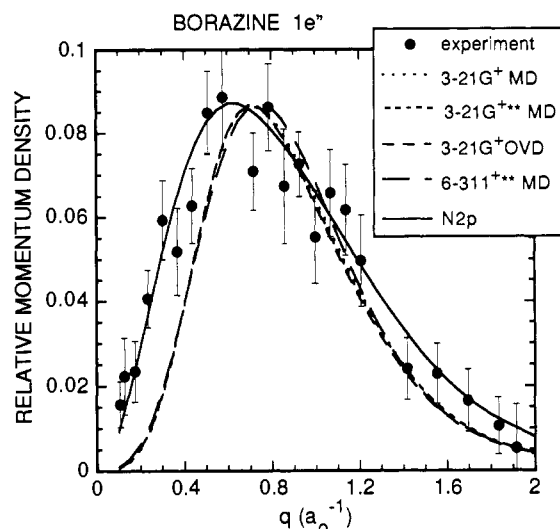


Figure 1. Experimental (e,2e) cross sections and calculated canonical molecular orbital momentum densities (MD) and neutral-cation overlap densities (OVD) for the HOMO of borazine.

identical to, the momentum density (MD) of the canonical molecular orbital (CMO) from which the electron has been ejected.

We focus only on the outermost MO with a binding energy of 10.1 eV. Although first identified as a σ orbital,⁸ later calculations showed conclusively that it is the $1e''$ π orbital.⁹ Our calculations confirm this result. The (e,2e) apparatus, with a resolution of 1.4 eV, cannot resolve the features observed in the photoelectron spectrum at 10.1, 11.4, and 12.8 eV that are identified with the three highest orbitals of borazine: the $1e''$ π orbital, the $6e'$ of σ character, and the $1a_2''$ π orbital, respectively (see ref 9 and our Table I). The three features merge into one broad peak in the (e,2e) binding energy spectrum; however, setting the instrument at 9.8 eV can separate the intensity associated with the 10.1-eV feature from the others. The measured (e,2e) cross section is shown in Figure 1. The measurement was initially compared to a calculated MD for the $1e''$ CMO represented by a 3-21G+** basis set. As shown in the Figure 1, the calculated density is significantly more narrow (smaller full width at half maximum) than the experimental measurement. To interpret this difference it is important to understand the relation between position space and momentum space representations. The momentum density is the square modulus of the momentum space wave function, which in turn is the Fourier transform of the position space wave function. The Fourier transformation of a function gives a function that bears an inverse relation to the original function. In other words, Fourier transformation of a compact function yields a diffuse function while transformation of a diffuse function gives a compact function. This leads to the initial conclusion that the $1e''$ electron density is significantly more compact in position space than predicted by the CMO calculation. To confirm this, a number of alternative explanations must be considered. These

(1) Robin, M. B. *J. Mol. Spectrosc.* **1978**, *70*, 472.
 (2) Doering, J. P.; Gedanken, A.; Hitchcock, A. P.; Fischer, P.; Moore, J.; Othoff, J. K.; Tossell, J.; Raghavachari, K.; Robin, M. B. *J. Am. Chem. Soc.* **1986**, *108*, 3602.
 (3) Boyd, R. J.; Choi, S. C.; Hale, C. C. *Chem. Phys. Lett.* **1984**, *112*, 136.
 (4) Cooper, D. L.; Wright, S. C.; Gerratt, J.; Hyams, P. A.; Raimondi, M. *J. Chem. Soc., Perkin Trans. 2* **1989**, 719.
 (5) McCarthy, I. E.; Weigold, E. *Phys. Rep.* **1976**, *27*, 275.
 (6) Moore, J. H.; Tossell, J. A.; Coplan, M. A. *Acc. Chem. Res.* **1982**, *15*, 192.
 (7) Brion, C. E. *Int. J. Quantum Chem.* **1986**, *29*, 1397.

(8) Frost, D. C.; Herring, F. G.; McDowell, C. A.; Stenhouse, I. A. *Chem. Phys. Lett.* **1970**, *5*, 291.
 (9) Anderson, W. P.; Edwards, W. D.; Zerner, M. C.; Canuto, S. *Chem. Phys. Lett.* **1982**, *88*, 185.